Parameter estimation of pharmacokinetics models in the presence of timing noise

Thierry Bastogne, Sophie Mézières-Wantz, Nacim Ramdani, Pierre Vallois, Muriel Barberi-Heyob

Parameter Estimation of Pharmacokinetics Models in the presence of Timing Noise

Thierry Bastogne, Sophie Mézières-Wantz, Nacim Ramdani, Pierre Vallois and Muriel Barberi-Heyob

***Abstract*— The problem addressed in this paper deals with the parameter estimation of *in vitro* uptake kinetics of drugs into living cells in presence of timing noise. Effects of the timing noise on the bias and variance of the output error are explicitly determined. A bounded-error parameter estimation approach is proposed as a suited solution to handle this problem. Application results are presented and emphasize its effectiveness in such an experimental framework.**

Keywords: parameter estimation, pharmacokinetics models, timing errors, bounded errors, biological systems.

I. INTRODUCTION

Pharmacokinetics is the study of the bodily absorption, distribution, metabolism and excretion of drugs by bodies. In chemical kinetics, reactions are generally described by differential equations which link the reaction rate with concentrations or pressures of reactants. In molecular cell biology, because of the complexity of systems, the nature of some reactions is still unclear. This paper is focused on the intracellular uptake kinetics of a photosensitizing drug (PS), *i.e.* the rate of photosensitizing molecules incorporated and accumulated by living cancer cells according to incubation terms [1]. The delivery control of the photosensitizing agent into the cancer cells is one the major factor on the therapeutic efficiency of the photodynamic therapy (PDT) [2]. Most of the PS uptake kinetics models are non-parametric, the temporal evolution of the PS intracellular concentration is described by step responses. The purpose of this study is the estimation of kinetics model parameters from data collected during *in vitro* kinetics experiments. These parameters are crucial information to both improve the modalities of the drug delivery process in photodynamic therapy and discriminate the uptake characteristics of different photosensitizers. Few papers have been reported for the application of system identification techniques to pharmacokinetics modeling problems [3]–[5].

T. Bastogne is with the Centre de Recherche en Automatique de Nancy (CRAN), Nancy-Université, CNRS, BP 239, F-54506 Vandœuvre-lès-Nancy Cedex, France thierry.bastogne@cran.uhp-nancy.fr

S. Mézières-Wantz and P. Vallois are with the Institut de Mathématiques Elie Cartan, Nancy-Université, CNRS, BP 239, F-54506 Vandœuvre-lès-Nancy Cedex, France sophie.wantz@iecn.u-nancy.fr, pierre.vallois@iecn.u-nancy.fr

N. Ramdani was with the CERTES EA 3481 Université Paris 12 Val de Marne. He is now with the Laboratoire d'Informatique, de Robotique et de Microélectronique de Montpellier (LIRMM) UMR CNRS 5506 Université de Montpellier 2, 161 rue Ada, 34392 Montpellier Cedex 5 - France. nacim.ramdani@lirmm.fr

M. Barberi-Heyob is with the Centre de Recherche en Automatique de Nancy (CRAN), Nancy-Université, CNRS, Centre Alexis Vautrin, 54511 Vandœuvre-lès-Nancy Cedex, France m.barberi@nancy.fnclcc.fr

Unfortunately, these approaches cannot be applied to the PS uptake kinetics. The intracellular PS concentration ($[P_i]$) is measured by a spectrofluorimeter but the latter induces a photobleaching process of the PS. The term photobleaching refers to the process by which the chromophoric structure of the PS is degraded by absorbed light energy [6]. As PS can be photobleached after light exposure, repeated experimentations for the same biological sample are not conceivable. In other terms, one biological sample with PS cannot be used for consecutive measurements of $[P_i]$. Collecting N_t data points of the kinetics then requires to repeat N_t times the same experiment (N_t biological samples) with identical initial conditions. To avoid the time consuming and the too high cost of such an experiment set up, N_t is generally kept small, *i.e.* $N_t \leq 10$. This limitation on N_t is the first problem to overcome for estimating kinetics parameters. The second difficulty is the low signal-to-noise ratio. The latter is due to a great measurement variability when working on living cells which are very sensitive to external disturbances. Thirdly, the choice of the stimulus signal is restricted to step signals which correspond to the amount of PS injected into the culture medium wells at time $t = 0$. A last issue is a timing offset error in the measurement samples. This timing error is bounded and can reach until $\pm 15mn$ for a measurement time sequence $\{t_j\} = \{1, 2, 4, 6, 8, 14, 18, 24h\}$. This error is not negligible and has rarely been taken into account in parameter estimation problems [7], particularly in this restricted experimental framework.

The problem addressed in this paper deals with the parameter estimation of pharmacokinetic models in presence of timing errors. Parameter estimation algorithms in system identification methods are often based on the minimization of a quadratic function of the output error, *i.e.* the difference between the system and the model outputs. The sensitivity of the output error to timing noise comparatively to input and output noise is unknown. The contributions of this paper are twofold:

- the stochastic effects of the timing noise on the output error are explicitly determined. They are compared with the ones of input and output noise. These results are obtained by assuming that there is no modeling error between the model and the biological system;
- a solution suited to this system identification problem is proposed and applied to *in vitro* data sets in a second part of this paper in order to assess its effectiveness in practice. The identification problem is addressed in the *bounded-error* context and is solved with a set pro-

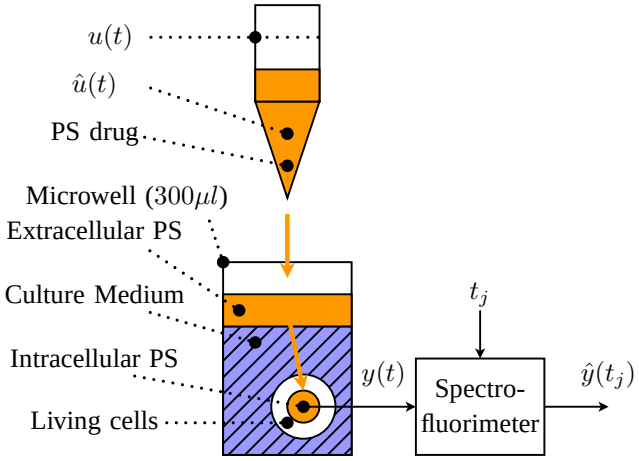

Fig. 1. *in vitro* experimental set up

jection algorithm based on interval analysis introduced in [8].

II. Experimental set up

TABLE I
Main notations

Symb.	Description
t	time variable
t_j	theoretical time instant associated with the j^{th} measurement sample
$\hat{t}_j$	real time instant associated with the j^{th} measurement sample
$u(t)$	noise-free input signal (stipulated by the experimenter)
$\hat{u}(t)$	real input signal
$y(t)$	system output variable (unknown by the experimenter)
$\hat{y}(t)$	measured output variable
$y_{\mathcal{M}}(t)$	model output variable
n_u	input noise
n_y	output noise
n_t	timing noise
$e_y(t)$	output error variable
$\mathcal{S}$	biological system
$\mathcal{M}(p)$	parametric model
p	vector of parameters
$N_t = card(\{t_j\})$	number of data points
N_r	number of repeated experiments at each time instant
x'	transposition of x
$\mathcal{N}(\mu, \sigma)$	gaussian distribution with mean μ and standard deviation σ
$\mathcal{U}(a, b)$	uniform distribution on the interval $[a; b]$
$\mathcal{E}\{\cdot\}$	mathematical expectation operator

Fig.1 depicts the basic material used in *in vitro* experiments for studying the uptake kinetics of a photosensitizing drug into living cells. Cells are seeded in $250\mu l$ culture wells and are exposed at time $t_0 = 0$ to a photosensitizing drug D. Let us consider the uptake phenomenon as a dynamic system. Its input variable $u(t)$ is a step signal which corresponds to the amount of drug injected into the well at time $t = 0$. Its output variable $y(t)$ is the amount of drug absorbed by the cells. $\hat{y}(t)$ is the measurement of $y(t)$ given by

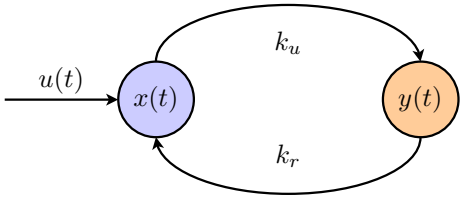

Fig. 2. *in vitro* compartmental model

a spectrofluorimeter at times $\{t_j\}$ with $j \in \{1, \cdots, N_t\}$. However, the spectrofluorimeter affects the biological state of the photosensitizing drug through a photobleaching process. Each culture well then becomes unusable after measurement. Consequently, to measure the intracellular PS concentration at N_t different time instants, it is necessary to repeat the same experiment in N_t different culture wells. Moreover, N_r identical wells are handled by the experimenter at each time instant t_j to *a posteriori* estimate the repeatability of the measurements. Globally, $N_r \times N_t$ wells are handled during the whole experiment. In practice, such an experiment is also repeated for other PS and different concentrations of protein in the medium. Consequently, the total number of wells to handle can be much larger than $N_r \times N_t$. All the wells are prepared in the same initial conditions.

III. *in vitro* PS uptake modeling

The *in vitro* uptake of the PS agent into cancer cells can be described by a compartmental modeling approach. In this paper, a linear two compartments model presented in Fig.2, is used. The two compartments are associated with the extracellular and intracellular volumes respectively. $x(t)$ denotes the amount of extracellular PS. Parameters k_u and k_r are the uptake and release rates respectively. Differential equations of this compartmental model are defined as follows

$$\frac{dx}{dt} = k_r y(t) - k_u x(t) + \frac{du}{dt} \quad (1)$$

$$\frac{dy}{dt} = k_u x(t) - k_r y(t), \quad (2)$$

with $x(0) = y(0) = 0$. After substitution of $x(t)$ from (1) in (2), it comes that

$$\frac{1}{k_u + k_r}\frac{dy}{dt} + y(t) = \frac{k_u}{k_u + k_r}u(t), \quad or \quad (3)$$

$$T\frac{dy}{dt} + y(t) = ku(t), \quad (4)$$

where $T = 1/(k_u + k_r)$ and $k = k_u/(k_u + k_r)$ are the time constant and the static gain of the PS uptake model described by a linear first-order differential equation. In [9], it is shown that a first-order transfer function is indeed a parsimonious model structure for describing the uptake kinetics of the *chlorin e6* photosensitizing drug into HT29-A4 cancer cells (human colon cancer cell line).

IV. Model and errors descriptions

The determination of a parametric model describing the uptake kinetics of a photosensitizing drug into living cells

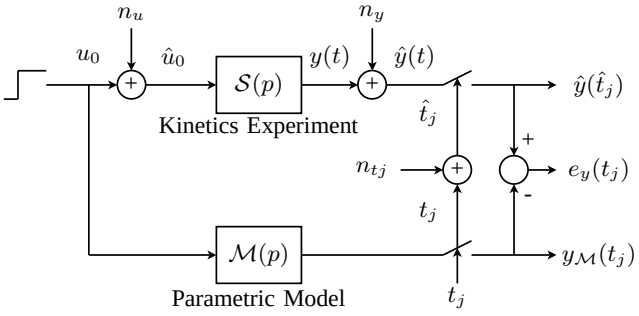

Fig. 3. Description of uncertainties

by extracting information from observations of u and y is a system identification problem [10]. At this point and thereafter, it is assumed that the system and the model are identical $\mathcal{M}(p) \equiv \mathcal{S}(p)$. However, as depicted in Fig. 3, three kinds of uncertainties are examined and are represented by output, input and timing noise (errors). Output and intput noise (n_y and n_u) are described by stationary stochastic processes added to the output and input signals. The timing noise (n_t) is a sequence of random variables added to the timing sequence $\{t_j\}$ controlling the sampling process of the output signal. $\hat{t}_j$ is the real time instant at which the output variable y is measured while t_j represents the theoretical measurement time instant noted by the experimenter. $e_y(t_j)$ denotes the output error between the system and the model outputs ($\hat{y}(\hat{t}_j)$ and $y_{\mathcal{M}}(t_j)$ respectively). Table I sums up the main notations used in the sequel.

A. Model structure

For the sake of simplicity, it is assumed in the sequel that $\mathcal{M}(p)$ and $\mathcal{S}(p)$ both rely on a first-order transfer function, inspired from (4),

$$\mathcal{S}(p): \quad T \cdot \frac{dy}{dt} + y(t) = k \cdot \hat{u}(t) \tag{5}$$

$$\mathcal{M}(p): \quad T \cdot \frac{dy_{\mathcal{M}}}{dt} + y_{\mathcal{M}}(t) = k \cdot u(t), \tag{6}$$

with $y(0) = y_{\mathcal{M}}(0) = 0$. $p = (T\,,\, k)$ is the parameter vector where T and k denote the time constant and the static gain respectively. From a biological point of view, T and k inform the biologist about the uptake rate and yield respectvely. $u(t)$ is a step signal of magnitude u_0 defined in (10). As a result, the intracellular concentration of the photosensitizing drug y follows a mono-exponential kinetics defined by

$$y(t) = k \cdot \hat{u}_0 \cdot (1 - e^{-t/T}). \tag{7}$$

B. Output noise

Conjugated effects of measurement noise and disturbances are usually described by a stochastic variable n_y added to y such that

$$\hat{y}(t_j) = y(t_j) + n_y(t_j), \tag{8}$$

where y and $\hat{y}$ denote the real biological response and its measurement respectively.

C. Input noise

u is a step signal defined by

$$u(t) = \begin{cases} 0 & t < 0 \\ u_0 & t \geq 0 \end{cases} \tag{9}$$

The step magnitude (u_0) represents the amount of the injected drug. The duration of injection is not significant compared to the duration of the experiment. The drug administration is usually carried out by multichannel micropipettes. For technical reasons, the real filling levels of drug in the cones are not identical and do not match with the dose stipulated by the experimenter. This error is represented by an input noise n_u added to u such that

$$\hat{u}(t) = \begin{cases} 0 & t < 0 \\ \hat{u}_0 = u_0 + n_u & t \geq 0 \end{cases} \tag{10}$$

where u_0 and $\hat{u}_0$ denote the prescribed dose and the effectively administrated dose respectively.

D. Timing noise

Each experimentation is carried out in a sterile framework in which each well is carefully handled by the experimenter. For each time instant t_j of the experimental set up, the living cells have to be washed, removed, lysed and diluted in ethanol by the experimenter. Such operations can take about $10mn$ during which each well, among the N_r ones, is individually handled. But the longest stage is the first one, i.e. the stage where the PS is administrated into all the wells; such an operation can take $20mn$. In practice, only the time instants t_j^- and t_j^+ corresponding to the beginning and the end of the experiment are noted by the experimenter. The nominal measurement time instant t_j noted by the experimenter in his table is an average time instant defined by $t_j = (t_j^+ + t_j^-)/2$. The real time instant $\hat{t}_j$ at which the uptake kinetics is stopped and measured, is unknown. This lack of precision in the timing of experiments is described by a timing noise n_t.

V. Stochastic modeling

In this section it is assumed that $\{n_y(t_j)\}$ is an independent and identically distributed sequence of Gaussian variables

$$n_y(t_j) = \sigma_y \cdot G_y^j, \tag{11}$$

where σ_y denotes the standard deviation of n_y and $G_y^j \approx \mathcal{N}(0,1)$. n_u is supposed to be a Gaussian variable defined by

$$n_u = \sigma_u \cdot G_u, \tag{12}$$

where σ_u denotes the standard deviation of n_u and $G_u \approx \mathcal{N}(0,1)$. The timing noise sequence $\{n_{tj}\}$ is supposed to be independent and identically distributed sequence of uniform variables such that

$$n_{tj} \approx \mathcal{U}(t_j^-, t_j^+) \tag{13}$$

$$\approx -\frac{\tau_j}{2} + \tau_j \cdot U_t^j, \tag{14}$$

with $\tau_j = t_j^+ - t_j^-$ and $U_t^j \approx \mathcal{U}(0,1)$. τ_j denotes the width of the timing uncertainty interval for the time instant t_j. $\{n_y(t_j)\}$, n_u and $\{n_{tj}\}$ are supposed to be independent. Given the previous assumptions about the input, output and timing noise, the expression of $e_y(t_j)$ becomes

$$e_y(t_j) = \hat{y}(\hat{t}_j) - y_{\mathcal{M}}(t_j) \tag{15}$$

$$= k \cdot (u_0 + \sigma_u G_u) \cdot (1 - e^{-\frac{1}{T}(t_j - \frac{\tau_j}{2} + \tau_j U_t^j)}) + \sigma_y G_y^j - k \cdot u_0 \cdot (1 - e^{-\frac{t_j}{T}}), \tag{16}$$

where k, T are given.

The mathematical expectation of $e_y(t_j)$ is defined in Proposition 5.1, its demonstration is developed in appendix II.

Proposition 5.1:

$$\mathcal{E}\{e_y(t_j)\} = k \cdot u_0 \cdot e^{\frac{-t_j}{T}} \left(1 - \textit{sinhc}(\frac{\tau_j}{2T})\right), \tag{17}$$

with $\textit{sinhc}(x) = \textit{sinh}(x)/x$ *denotes the hyperbolic sinus cardinal function of* x.

Since $x \rightarrow \text{sinhc}(x)$ is increasing on $\mathbb{R}^+$, equation (17) shows that $\mathcal{E}\{e_y(t_j)\} < 0$. This systematic bias is only due to the timing noise. The absolute value of the mean output error increases with respect to τ and is null only for $\tau = 0$.

The variance of $e_y(t_j)$ is given in Proposition 5.2, its demonstration is developed in appendix III.

Proposition 5.2:

$$Var\{e_y(t_j)\} = \sigma_y^2 + k^2\sigma_u^2 + k^2 e^{\frac{-t_j}{T}} \cdot \textit{sinhc}(\frac{\tau_j}{2T})(A + B), \tag{18}$$

with: $A = e^{\frac{-t_j}{T}} \left(\cosh(\frac{\tau_j}{2T}) - \textit{sinhc}(\frac{\tau_j}{2T})\right) u_0^2$ *and* $B = \left(e^{\frac{-t_j}{T}} \cosh(\frac{\tau_j}{2T}) - 2\right) \sigma_u^2$.

To take into account both the bias and the variance of $e_y(t_j)$, its mean square error defined by $\varepsilon(t_j) = \mathcal{E}^2\{e_y(t_j)\} + Var\{e_y(t_j)\}$ is examined thereafter. Three specific values of $\varepsilon(t_j)$, noted $\varepsilon_{ny}(t_j)$, $\varepsilon_{nu}(t_j)$ and $\varepsilon_{nt}(t_j)$, are determined to emphasize the contribution of each kind of noise.

- $\sigma_u = 0$, $\tau_j = 0$:

$$\varepsilon_{ny}(t_j) = \sigma_y^2, \tag{19}$$

- $\sigma_y = 0$, $\tau_j = 0$:

$$\varepsilon_{nu}(t_j) = k^2\sigma_u^2 \left(e^{\frac{-t_j}{T}} - 1\right)^2, \tag{20}$$

- $\sigma_y = 0$, $\sigma_u = 0$:

$$\varepsilon_{nt}(t_j) = k^2 u_0^2 e^{\frac{-2t_j}{T}} \left(1 - 2\text{sinhc}(\frac{\tau_j}{2T}) \right. \tag{21}$$

$$\left. + \text{sinhc}(\frac{\tau_j}{2T}) \cosh(\frac{\tau_j}{2T})\right). \tag{22}$$

The effect of the timing noise on the output error is estimated as significant if there exists a time instant t_j such that $\varepsilon_{nt}(t_j) > (\varepsilon_{nu}(t_j) + \varepsilon_{ny}(t_j))/10$. For instance, if $u_0 = 1, k = 0.3, T = 5, t_j = 1, \tau_j = 0.5, \sigma_y = 0.01, \sigma_u = 0.1$[1] then $\varepsilon_{nt}(t_j) \approx 5 \cdot 10^{-5}$, $\varepsilon_{nu}(t_j) \approx 3 \cdot 10^{-5}$ and $\varepsilon_{ny}(t_j) \approx 1 \cdot 10^{-4}$. Consequently, the effect of the timing noise on the output error cannot be neglected for the time instant $t_j = 1\,(h)$. The impact of n_t decreases as t_j and becomes negligible from $t_j \gtrsim 3\,(h)$. This example emphasizes that n_t could significantly influence the estimation of the time constant which mainly depends on the first measurement samples. Since the consequences of n_t cannot be reasonably ignored, usual parameter estimation methods (those assuming only the presence of output noise) and error-in-variables approaches are not appropriate to solve this estimation problem. In the next section, a bounded-error parameter estimation approach is proposed as a suited solution to handle timing errors.

[1]These values have been chosen from empirical knowledge of biologists and experimental results reported in [11].

VI. Bounded-error estimation with *in vitro* data

Bounded-error or set-membership approaches allow to estimate parameters and their uncertainty in inverse problem contexts in which all uncertain quantities are assumed as unknown but bounded with known bounds. No further hypothesis about probability distributions is stated. Several algorithms have been developped to solve estimation problems stated in the bounded-error context. When models are non linear, most approaches use interval analysis and constraint propagation techniques. Allied with global algorithms and a reliable numerical implementation, they derive guaranteed computations, i.e. they provide a numerical proof of property or non-property. They are rather mature techniques and have already been successfully applied for solvling problems in biology, chemical or thermal engineering, economics, computer vision or robotics, when guaranteed computations were essential [8], [12].

In this part, we assume that all the uncertain quantities satisfy this *bounded-error* property and bounded-error estimation techniques are applied to experimental data collected during *in vitro* uptake kinetics experiments of a PS into human malignant glioma cells. The experimental protocol is defined by $N_t = 5$, $N_r = 6$ and $u_0 = 25mol$.

TABLE II

Prior feasible intervals for the data

j	t_j (h)	$[t_j]$	$[\hat{y}(t_j)]$
1	1	[0.67;1.33]	[0;0.607]
2	2	[1.67;2.33]	[0.238;0.861]
3	8	[7.67;8.33]	[0.681;1.396]
4	18	[17.67;18.33]	[0.661;1.447]
5	24	[23.67;24.33]	[1.376;2.459]

Fig. 4 presents the experimental data of six PS uptake kinetics carried out in the same experimental framework. Each cross corresponds to one measurement. The output variable measured by the spectrofluorimeter is given in arbitrary unit. Prior intervals $[\hat{y}(t_j)]$ and $[t_j]$ on the output measurements and the time instants are given in table II. Bounds of $[t_j]$ have been measured during the kinetics experiment. $[\hat{y}(t_j)]$ has been determined from the minimum and maximum values of measurements. The uncertainty associated with each pair of output and time data is materialized by a box. The set $\widehat{\mathbb{P}}$

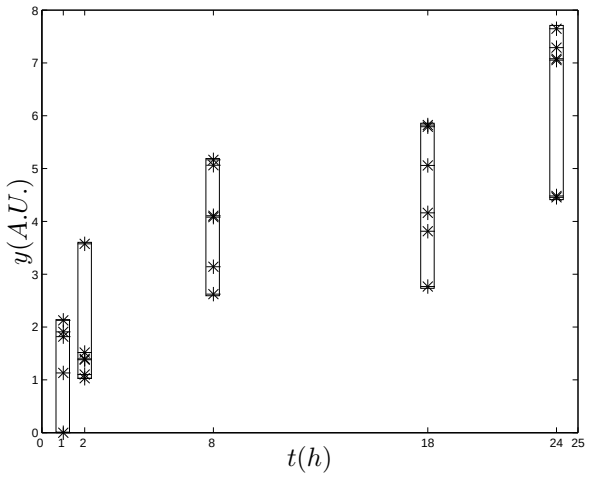

Fig. 4. Experimental data, intervals and boxes

to be characterized consists of all the values of $\mathbf{p} = (k, T)'$ such that the graph of the function

$$g(\mathbf{p}, t) = k \cdot u_0 \cdot (1 - e^{-t/T}) \tag{23}$$

goes through all five boxes of Fig. 4. $\widehat{\mathbb{P}}$ is defined as

$$\widehat{\mathbb{P}} = \{\mathbf{p} \in \mathbb{R}^{+2} | \exists \mathbf{t} \in \mathbb{R}^{+5}, (g(\mathbf{p}, \mathbf{t}), \mathbf{p}, \mathbf{t}) \in \mathbb{X}\} \tag{24}$$

with

$$g(\mathbf{p}, \mathbf{t}) = \begin{pmatrix} g(\mathbf{p}, t_1) & \cdots & g(\mathbf{p}, t_{N_t}) \end{pmatrix}, \tag{25}$$

and

$$\mathbb{X} = [\hat{y}(t_1)] \times \cdots \times [\hat{y}(t_5)] \times [\check{k}] \times [\check{T}] \times [t_1] \times \cdots \times [t_5], \tag{26}$$

and the prior box for the parameters given by

$$\check{\mathbb{P}} = [\check{k}] \times [\check{T}] = [1, 4] \times [1, 40]. \tag{27}$$

$\widehat{\mathbb{P}}$ can be estimated in a guaranteed way using a set inversion algorithms based on parameter space partionning, interval analysis and constraint propagation techniques (see [8] and the references therein). Fig. 5 presents the estimate of $\widehat{\mathbb{P}}$ when the partionning algorithm is set not to partition boxes with a size smaller than 0.01

In Fig. 5, the paving form associated with $\widehat{\mathbb{P}}$ is composed of grey and black boxes. The grey boxes have been proved to be included in $\mathbb{P}$ but no conclusion has been reached for the black ones. The external envelope of $\widehat{\mathbb{P}}$ is defined by $\hat{k} \in [1.37; 3.49]$ and $\hat{T} \in [1.7; 33]$. This results shows that the estimation uncertainty on the time-constant is larger than the one on the static gain. Fig. 6 depicts the *a posteriori* estimate of the output set $\widehat{\mathbb{Y}}$, a set of time trajectories defined by

$$\widehat{\mathbb{Y}} = \Big\{(t, y) \in \mathbb{R}^+ \times \mathbb{R} | \, y(t) = k u_0 (1 - e^{-t/T}), \text{ with } (k, T)^T \in \widehat{\mathbb{P}}\Big\}. \tag{28}$$

This figure points out a wide variation of the initial slope of the step response which explains the large uncertainty on the time-constant estimate. In this study case, the wide variation

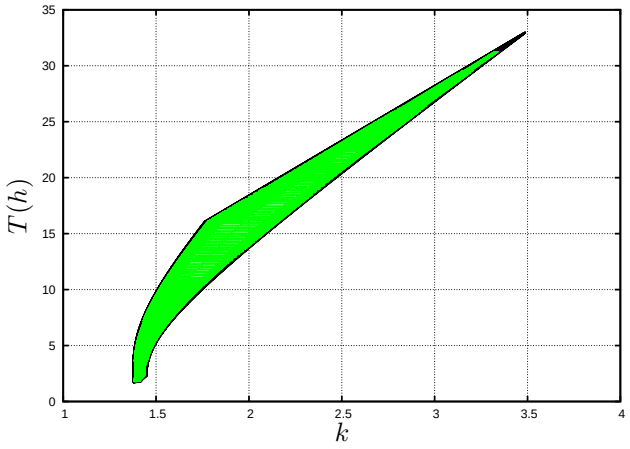

Fig. 5. *a posteriori* estimate of the parameter set $\widehat{\mathbb{P}}$

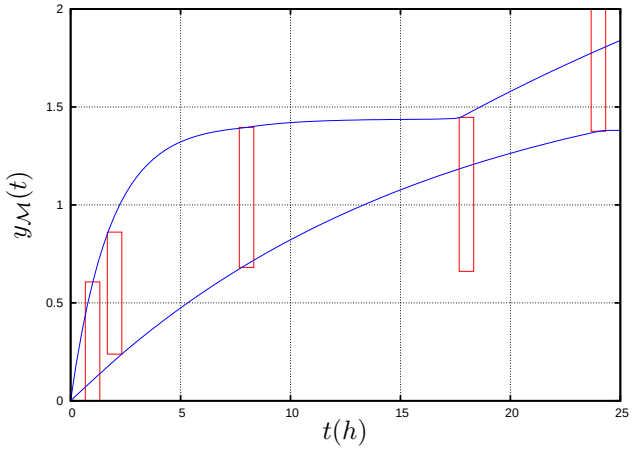

Fig. 6. *a posteriori* estimate of the output set $\widehat{\mathbb{Y}}$

of the initial slope is mainly due to the height of the boxes rather than their width. In other terms, in this application, the uncertainty on the time-constant estimate is mainly caused by the output noise rather than the timing noise.

VII. Conclusion

This paper focuses on consequences of timing errors in collected data on the parameter estimation of kinetics models and more precisely their effects on the output error. The contribution of the timing noise on the output error is compared with the ones induced by input and output noise in terms of bias and variance. Mathematical expressions of the bias and variance of the output error with respect to the parameters of input, output and timing noises are established. It is shown that the influence of the timing noise on the output error can be significant, particularly for the first measurement time instants ($t_j \lesssim 3\,h$). An application to *in vitro* data is developed in the second part of this paper. It is shown how the timing noise can be taken into account by bounded-error estimation algorithms based on interval analysis. The timing noise is described as a bounded error and no further hypothesis about probability distributions is stated. The results presented herein emphasize the effectiveness of such an

bounded-error estimation approach in such an experimental framework.

REFERENCES

[1] M. Barberi-Heyob, P.-O. Védrine, J.-L. Merlin, R. Millon, J. Abecassis, M.-F. Poupon, and F. Guillemin, "Wild-type p53 gene transfer into mutated p53 HT29 cells improves sensitivity to photodynamic therapy via induction of apoptosis," *Int. J. Oncol.*, no. 24, pp. 951–958, 2004.

[2] J. G. Moser, *Photodynamic Tumor Therapy: 2nd and 3rd Generation*. Gordon & Breach Science Publishers, 1998.

[3] N. D. Evans, R. J. Errington, M. J. Chapman, P. J. Smith, M. J. Chappell, and K. R. Godfrey, "Compartmental modelling of the uptake kinetics of the anti-cancer agent topotecan in human breast cancer cells," *International Journal of Adaptive Control and Signal Processing*, vol. 19, pp. 395–417, 2005.

[4] C. L. Beck, H.-H. Lin, and M. Bloom, "Multivariable modeling and control of anesthetic pharmacodynamics," in *Proc of the CNRS-NSF Workshop on Biology and Control Theory: current challenges*, Toulouse, France, April 2006.

[5] R. Ali, L. Campbell, N. D. Evans, R. J. Errington, K. R. Godfrey, P. J. Smith, and M. J. Chappell, "A PK-PD model of cell cycle response to topotecan," in *Proc of the IFAC Modelling and Control in Biomedical Systems*, Reims, France, September 2006, pp. 477–482.

[6] M. J. Niedre, A. J. Secord, M. S. Patterson, and B. C. Wilson, "*In vivo* tests of the validity of singlet oxygen luminescence measurements as a dose metric in photodynamic therapy," *Cancer Research*, vol. 63, pp. 7986–7994, november 2003.

[7] J. Kusuma and V. K. Goyal, "Signal parameter estimation in the presence of timing noise," in *Proc of the 40th Conference on Information Science and Systems, CISS'06*, Princeton, NJ, USA, March 2006.

[8] L. Jaulin, M. Kieffer, O. Didrit, and E. Walter, *Applied Interval Analysis*. Springer, 2001.

[9] T. Bastogne, L. Tirand, M. Barberi-Heyob, and A. Richard, "Modélisation système de la thérapie photodynamique," in *4ème Conférence Internationale Francophone d'Automatique*, Bordeaux, France, May-June 2006.

[10] E. Walter and L. Pronzato, *Identification of Parametric Models from experimental data*. Springer-Verlag, Masson, 1997.

[11] T. Bastogne, L. Tirand, M. Barberi-Heyob, and A. Richard, "System identification of photosensitiser uptake kinetics in photodynamic therapy," in *Proc of the 6th IFAC Symposium on Modelling and Control in Biomedical System (including biological systems)*, Reims, France, Sept. 2006.

[12] I. Braems, N. Ramdani, M. Kieffer, L. Jaulin, E. Walter, and Y. Candau, "Guaranteed characterization of thermal conductivity and diffusivity in presence of model uncertainty," accepted in *Inverse Problems in Science and Engineering*, 2006.

APPENDIX I

Lemma 1.1:

$$\mathcal{E}\{e^{a(\frac{1}{2}-U)}\} = \frac{\sinh(\frac{a}{2})}{\frac{a}{2}} = \text{sinhc}\left(\frac{a}{2}\right), \tag{29}$$

where a is a non-null constant and U is a random variable distributed according to a uniform law on $[0,1]$.

APPENDIX II
PROOF OF THE PROPOSITION 5.1

Proof: Since G_u and G_y^j are centered and since U_t^j and G_u are independent, then

$$\begin{aligned}
\mathcal{E}\{e_y(t_j)\} &= k\cdot u_0 \cdot \left(1 - \mathcal{E}\{e^{-\frac{1}{T}(t_j - \frac{\tau_j}{2} + \tau_j U_t^j)}\}\right) \\
&\quad - k\cdot u_0 \cdot \left(1 - e^{-\frac{t_j}{T}}\right) && (30)\\
&= k\cdot u_0 \cdot e^{-\frac{t_j}{T}} \left(1 - \mathcal{E}\{e^{-\frac{1}{T}(-\frac{\tau_j}{2} + \tau_j U_t^j)}\}\right) && (31)\\
&= k\cdot u_0 \cdot e^{-\frac{t_j}{T}} \left(1 - \mathcal{E}\{e^{\frac{\tau_j}{T}(\frac{1}{2} - U_t^j)}\}\right). && (32)
\end{aligned}$$

It can be deduced from Lemma 1.1 that

$$\mathcal{E}\{e_y(t_j)\} = k\cdot u_0 \cdot e^{-\frac{t_j}{T}} \left(1 - sinhc(\frac{\tau_j}{2T})\right). \tag{33}$$

■

APPENDIX III
PROOF OF THE PROPOSITION 5.2

Proof: From (16), $e_y(t_j)$ is rewritten such that

$$e_y(t_j) = X_1 + X_2 - y_{\mathcal{M}}(t_j), \tag{34}$$

with

$$\begin{aligned}
X_1 &= k\cdot(u_0 + \sigma_u G_u)\cdot(1 - e^{-\frac{1}{T}(t_j - \frac{\tau_j}{2} + \tau_j U_t^j)}) && (35)\\
X_2 &= \sigma_y G_y^j. && (36)
\end{aligned}$$

Since X_1 and X_2 are independent, it can be deduced that

$$\begin{aligned}
Var(e_y(t_j)) &= Var(X_1) + Var(X_2) && (37)\\
&= Var(X_1) + \sigma_y^2. && (38)
\end{aligned}$$

Let us compute the expectation of X_1.

$$\begin{aligned}
\mathcal{E}\{X_1\} &= k\cdot u_0 \cdot \left(1 - e^{\frac{-t_j}{T}} \mathcal{E}\{e^{\frac{\tau_j}{T}(\frac{1}{2} - U_t^j)}\}\right) && (39)\\
&= k\cdot u_0 \cdot \left(1 - e^{\frac{-t_j}{T}} sinhc(\frac{\tau_j}{2T})\right), && (40)
\end{aligned}$$

according to Lemma 1.1. The expectation of X_1^2 is given by

$$\begin{aligned}
\mathcal{E}\{X_1^2\} &= k^2 \mathcal{E}\{(u_0 + \sigma_u G_u)^2\}\mathcal{E}\{X_3^2\} && (41)\\
&= k^2(u_0^2 + \sigma_u^2)\mathcal{E}\{X_3^2\}, && (42)
\end{aligned}$$

where

$$X_3 = 1 - e^{-\frac{1}{T}(t_j - \frac{\tau_j}{2} + \tau_j U_t^j)}. \tag{43}$$

We have

$$\begin{aligned}
\mathcal{E}\{X_3^2\} &= 1 + \mathcal{E}\{e^{-\frac{2}{T}(t_j - \frac{\tau_j}{2} + \tau_j U_t^j)}\} - 2\mathcal{E}\{e^{-\frac{1}{T}(t_j - \frac{\tau_j}{2} + \tau_j U_t^j)}\} \\
&= 1 + e^{-\frac{2t_j}{T}} \mathcal{E}\{e^{\frac{2\tau_j}{T}(\frac{1}{2} - U_t^j)}\} - 2e^{-\frac{t_j}{T}} \mathcal{E}\{e^{\frac{\tau_j}{T}(\frac{1}{2} - U_t^j)}\} \\
&= 1 + e^{-\frac{2t_j}{T}} sinhc(\frac{\tau_j}{T}) - 2e^{-\frac{t_j}{T}} sinhc(\frac{\tau_j}{2T}). && (44)
\end{aligned}$$

We finally obtain

$$\begin{aligned}
Var\{X_1\} &= k^2(u_0^2 + \sigma_u^2)\left(1 + e^{-\frac{2t_j}{T}} sinhc(\frac{\tau_j}{T})\right. \\
&\quad \left. -2e^{-\frac{t_j}{T}} sinhc(\frac{\tau_j}{2T})\right) - k^2 u_0^2 \left(1 - e^{-\frac{t_j}{T}} sinhc(\frac{\tau_j}{2T})\right)^2 \\
&= k^2(u_0^2 + \sigma_u^2)\left(1 + e^{-\frac{2t_j}{T}} sinhc(\frac{\tau_j}{T}) - 2e^{-\frac{t_j}{T}} sinhc(\frac{\tau_j}{2T})\right) \\
&\quad - k^2 u_0^2 \left(1 - 2e^{-\frac{t_j}{T}} sinhc(\frac{\tau_j}{2T}) + e^{-\frac{2t_j}{T}} \left(sinhc(\frac{\tau_j}{2T})\right)^2\right) \\
&= k^2 \left(\sigma_u^2 + (u_0^2 + \sigma_u^2) e^{-\frac{2t_j}{T}} sinhc(\frac{\tau_j}{T})\right. \\
&\quad \left. -2\sigma_u^2 e^{-\frac{t_j}{T}} sinhc(\frac{\tau_j}{2T}) - u_0^2 e^{-\frac{2t_j}{T}} \left(sinhc(\frac{\tau_j}{2T})\right)^2\right). && (45)
\end{aligned}$$

Equation (18) in proposition 5.2 is then a direct consequence of (38).

■